ELSEVIER

Contents lists available at ScienceDirect

# International Journal of Applied Earth Observation and Geoinformation

journal homepage: www.elsevier.com/locate/jag



# Insights into spatiotemporal dynamics and driving mechanisms of vegetation net primary productivity in African terrestrial ecosystems<sup>★</sup>

Liang Liang \*0, Meng Li, Ziru Huang, Qianjie Wang, Zhen Yang, Shuguo Wang

School of Geography, Geomatics and Planning, Jiangsu Normal University, Xuzhou 221116, China

#### ARTICLE INFO

Keywords:
Africa
NPP
Wavelet analysis
Hurst exponent
Structural equation model

#### ABSTRACT

Net Primary Productivity (NPP) is a critical measure of ecosystem vitality. This paper examines the spatiotemporal variation in NPP across Africa during 1981-2018 using Theil-Sen slope estimation and wavelet analysis. Sustainable change characteristics in different regions are analyzed using the Hurst exponent, and the influence of driving factors on African NPP are quantified through a structural equation model (SEM). The analysis revealed that: (1) The annual variation curve of African NPP demonstrated a fluctuating upward trajectory (p = 0.001) throughout the study period. Wavelet analysis revealed a cyclical pattern with a primary period of about 20 years, characterized by two upward and downward transitions during 1981-2018. (2) Spatial analysis indicates the distribution of NPP across Africa is centered around the equator and gradually decreases towards higher latitudes, in which the NPP of tropical rainforest and its adjacent areas increases significantly, covering 40.2 % of Africa's area. However, Hurst exponent analysis reveals that NPP in Africa generally exhibits antisustainability changes, with 52.8 % of the total area potentially shifting from growth to decline in the future. (3) SEM analysis shows that NPP in Africa is mainly regulated by natural factors, particularly cumulative precipitation and temperature extremes, which exhibit the highest impact coefficient of 0.89. While topographic factors also have a substantial overall effect, their impact is primarily indirect through climate, with minimal direct influence. These findings offer a scientific foundation and policy support for sustainable development of environmental and socio-economic systems in Africa.

#### 1. Introduction

Vegetation's Net Primary Productivity (NPP) is an essential indicator of the productivity of plant communities and reflects their capacity to sequester  $CO_2$  (Field et al., 1998; Mao et al., 2024). Variations in NPP signify vegetation's response to environmental changes, providing a vital foundation for evaluating regional carbon sink potential and sustainable development (Chen et al., 2024; Liang et al., 2023; Wang et al., 2023b).

Africa, with its diverse geographical and ecological land-scapes—ranging from vast grasslands and arid deserts to lush tropical rainforests—boasts rich biodiversity. However, the continent's ecological environment is relatively fragile due to high temperatures and limited water resources. Despite Africa's low CO<sub>2</sub> emissions, the continent disproportionately suffers from climate change impacts, facing challenges such as desertification, soil degradation, water scarcity, and

agricultural disruption (Jin et al., 2022; Yadou et al., 2024). The continent's terrestrial ecosystems demonstrate low adaptability and high susceptibility to climate change, significantly affecting vegetation growth and NPP, especially amid rising human activities (Espoir et al., 2024; Yadou et al., 2024). Therefore, a thorough evaluation of ecological conditions, including vegetation NPP in African terrestrial ecosystems, is crucial to understand the status and sustainability of these ecosystems.

Enhancing terrestrial carbon sequestration capacity is a priority for initiatives like the African Union's "Great Green Wall" and the United Nations' "2030 Sustainable Development Goals". Recent research on the spatiotemporal dynamics of African NPP has made notable strides. Remote sensing and statistical modeling indicate a sustained NPP decline in the Sahel due to reduced precipitation and overgrazing (Brandt et al., 2017), while adaptive vegetation responses to rainfall fluctuations have led to localized recovery in East African savannas

E-mail address: liang\_rs@jsnu.edu.cn (L. Liang).

<sup>\*</sup> This article is part of a special issue entitled: 'African EO – Mapping - Invited' published in International Journal of Applied Earth Observation and Geoinformation.

<sup>\*</sup> Corresponding author.

(Hutley et al., 2022). Methodologies including correlation analysis, multiple regression, and machine learning are widely used to examine the direct impacts of climatic variables (e.g., precipitation, temperature) and human activities (e.g., cropland expansion) on NPP (Igboeli et al., 2025; Maluleke, et al., 2025; Tong, et al., 2019).

However, most studies focus on specific regions or time periods, lacking a comprehensive analysis of long-term NPP changes across the continent. This limitation makes it difficult to differentiate between short-term fluctuations and long-term degradation trends in NPP, complicating site selection and priority determination for ecological restoration projects (Igboeli et al., 2025; Tong et al., 2019). Furthermore, research predominantly emphasizes historical trend analysis, with insufficient assessment of the persistence (e.g., reversibility/irreversibility) of future NPP changes. This gap hinders the development of forward-looking ecological restoration policies and long-term risk management strategies (Berdugo et al., 2020). Additionally, while some studies attempt to elucidate the driving mechanisms behind NPP variations, they often rely on linear statistical models (e.g., Pearson correlation analysis, multiple linear regression). These models are inadequate for capturing nonlinear synergistic effects among drivers (e.g., interactions between topography and human activities) or identifying potential mediating pathways (e.g., indirect climatic effects moderated by terrain). Consequently, management measures based on such studies (e.g., large-scale afforestation) may overlook critical indirect effects and nonlinear feedbacks, potentially reducing their effectiveness (Liu et al., 2022a; Veldman et al., 2015; Wang et al., 2020). Hence, it is imperative to develop an integrated NPP analysis framework that combines "spatiotemporal variation analysis, persistence assessment, and mechanistic interpretation" to provide scientifically rigorous and policyrelevant decision support for African ecological restoration (Turner et al., 2020).

This study utilizes long-term NPP data to address the following topics in Africa: (1) examining the spatiotemporal dynamics pattern of African NPP from 1981 to 2018; (2) analyzing historical trends and assessing future characteristics of NPP in Africa through trend and sustainability analyses; and (3) evaluating the effects of both natural and humaninduced factors on NPP variations across Africa and exploring the underlying mechanisms. The results aim to assist Africa in formulating sustainable ecological and environmental protection policies.

#### 2. Research area

Africa (37°21'N-34°51'S and 51°24'E-17°33'W) exhibits an arid climate with limited rainfall and can be categorized into five parts (Fig. 1). The equator runs through the central region, and both temperature and rainfall reduce progressively away from the equator. This climatic zonality and symmetry are reflected in the distribution of vegetation. Near the equator, in the Congo Basin and along the Gulf of Guinea, tropical evergreen rainforests prevail due to year-round heat and rainfall. Moving north and south from the equator, the dry season lengthens, rainfall diminishes, and vegetation transitions through deciduous forests, shrubs, and grasslands. Due to high temperatures and aridity, the Sahara and western Kalahari regions are characterized by sparse vegetation. On the southeastern coast of Africa and eastern Madagascar, southeast trade winds and mountainous terrain create tropical forests on windward slopes and savannah landscapes on leeward slopes, highlighting an east-to-west vegetation gradient (White, 1983; Nicholson, 2017).

#### 3. Research data

#### 3.1. NPP data

The NPP data utilized in this research, spanning from 1981 to 2018 with a spatial resolution of 5 km and an 8-day temporal interval, were obtained from the National Earth System Science Data Center (NESSDC) of China (available at: https://www.geodata.cn). This dataset was produced using the MuSyQ-NPP model (Liu et al., 2021a; Yu et al., 2018), which incorporates inputs from GLASS LAI and FPAR products, MODIS land cover data, and ERA-Interim meteorological reanalysis. The accuracy of the NPP product was validated against independent observations from the FLUXNET network (Liu et al., 2021a; Yu et al., 2018). For temporal aggregation, this research employs Maximum Value Compositing (MVC) for monthly data and Mean Synthesis for annual data.

# 3.2. Land cover data

The GLC\_FCS30-2020 dataset (Liu et al., 2021b; Zhang et al., 2020; Zhang et al., 2021) was employed to categorize the various ecosystems throughout Africa. This dataset offers a comprehensive and dynamic monitoring of land cover from 1985 to 2020, comprising 9 primary

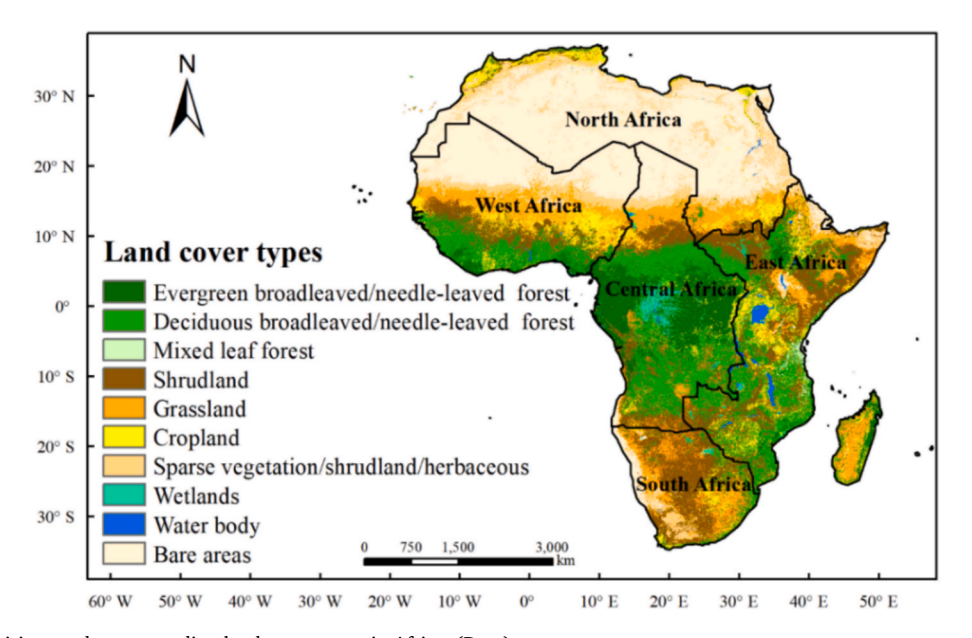


Fig. 1. Geographical divisions and corresponding land cover types in Africa. (Data). Source: GLC FCS30-2020 dataset

categories and 30 distinct subcategories. However, as the classification system is designed for global land cover, some types are underrepresented in the African context. To more accurately depict the African ecosystem, similar land cover categories were merged into 10 consolidated types based on the classification framework proposed by Chen et al. (2015) and Gong et al. (2019) (see Fig. 1).

#### 3.3. Various driving factor data

This study utilizes SEM model to examine the interactions between NPP and both natural and human-induced factors.

The natural factors include climatic variables (precipitation and temperature—mean, maximum, and minimum) and topographic features (elevation, slope, and aspect). The monthly climate dataset for the research period, with a spatial resolution of 2.5 arc-minutes, was obtained from NESSDC (https://www.geodata.cn). Annual mean climate datasets were then generated by averaging the monthly data. Topographic data were sourced from the Shuttle Radar Topography Mission (SRTM) Digital Elevation Model (DEM), which has an original spatial resolution of 60 arc-seconds.

The human-induced factors encompass gross domestic product (GDP), industrial structure, and population density. Relevant statistical data for the study period were sourced from the World Bank database (https://data.worldbank.org). These point-based statistical data were transformed into continuous raster surface data using the spatial interpolation capabilities of ArcGIS 10.8 software.

To ensure consistency in spatial resolution across all input variables for the SEM analysis, all driving factor datasets were uniformly resampled to a  $0.5^{\circ} \times 0.5^{\circ}$  grid scale using bilinear interpolation. At this uniform resolution, the total number of valid pixels covering Africa was 10,239 for each time period.

# 4. Research method

# 4.1. Interannual variation of NPP and wavelet analysis

Time-series NPP data were processed with the MVC method to generate monthly composites that reduce cloud and atmospheric effects. Annual NPP was then derived by averaging the monthly composites, thereby enabling analysis of interannual variability at the continental scale.

To conduct an in-depth examination of the periodic oscillation in NPP interannual variation, we applied wavelet transform, hailed as the mathematical microscope. Specifically, we used Morlet wavelet analysis to investigate the temporal periodic patterns of long-term NPP time series across Africa. Being a complex continuous wavelet, the Morlet wavelet is adept at capturing temporal or frequency variations in signals, making it particularly suitable for analyzing non-stationary signals. The Morlet mother wavelet is mathematically expressed as follows (Ghaderpour et al., 2023):

$$\varphi(t) = \pi^{-\frac{1}{4}} e^{-iw_0 t} e^{-\frac{t^2}{2}} \tag{1}$$

The wave function  $\varphi(t)$  is derived from the combination of the complex sine function  $e^{-iw_0t}$  and the Gaussian wave packet  $e^{-\frac{t^2}{2}}$ . The normalization factor  $\pi^{-\frac{1}{4}}$  ensures unit variance, while t and  $w_0$  denote dimensionless time and frequency, respectively. This research employs annual average NPP data to examine the overarching periodic patterns of African NPP on a continental scale via Morlet wavelet analysis.

# 4.2. Distribution pattern and trend analysis

To investigate the spatial distribution pattern of African NPP, we computed the multi-year mean for the period 1981–2018, producing a spatial distribution map spanning 38 years. To further delineate its

spatiotemporal evolution characteristics, we employed the Theil-Sen slope estimator to identify trends at the pixel level and the Mann-Kendall test to assess their statistical significance. These methods, which involve slope variation and rank-based analysis, provide distinct advantages, such as no requirement for prior distributional assumptions, robustness against outliers, and compatibility with non-normally distributed data (Gocic and Trajkovic, 2013; Wang et al., 2023a; Yue et al., 2002).

# 4.2.1. Theil-Sen slope estimation

The Theil-Sen estimator is a robust and simple technique ideal for trend analysis in time-series data (Wang et al., 2023b). To examine the overall trends in NPP from 1981 to 2018, the Theil-Sen slope was calculated from the annual NPP values for each pixel during the study period (Gocic and Trajkovic, 2013):

$$Sen = Median\left(\frac{NPP_j - NPP_i}{j - i}\right), \ \forall j > 1$$
 (2)

Here, the Median refers to the median of the calculated sequence values;  $NPP_i$  and  $NPP_j$  stand for the NPPs for the i-th and j-th years, respectively. A positive Sen means an increase, whereas a negative Sen suggests a decline.

#### 4.2.2. Mann-Kendall trend test

The integrated use of the Mann-Kendall test and the Theil-Sen estimator (Liang et al., 2022; Yue et al., 2002) provides an effective means to quantify spatiotemporal variability. This research applies this integrated methodology to assess the trend of NPP time series at the pixel level and produces a significance classification map of NPP trend alterations through statistical significance analysis.

For NPP series  $NPP_1, NPP_2, \cdots, NPP_n$  with n sample sizes, the magnitude relationship between  $NPP_i$  and  $NPP_j$  ( $NPP_i, NPP_j, j > i$ ) in all dual values is initially determined. Subsequently, the statistic S can be computed as outlined by (Güçlü, 2020):

$$S = \sum_{i=1}^{n-1} \sum_{i=i+1}^{n} Sgn(NPP_{j} - NPP_{i})$$
 (3)

where Sgn represents the sign function, computed as:

$$Sgn(NPP_{j}-NPP_{i}) = \begin{cases} +1, NPP_{j} > NPP_{i} \\ 0, NPP_{j} = NPP_{i} \\ -1, NPP_{j} < NPP_{i} \end{cases}$$

$$(4)$$

For n > 8, the random sequence S is well-approximated by a Gaussian distribution, and the trend analysis utilizes the test statistic Z, defined as follows:

$$Z = \begin{cases} \frac{S-1}{\sqrt{Var(S)}}, (S>0) \\ 0, (S=0) \\ \frac{S+1}{\sqrt{Var(S)}}, (S<0) \end{cases}$$
 (5)

In this equation, Var(S) is the variance, and the calculation formula is:

$$Var(S) = \frac{n(n-1(2n+5))}{18}$$
 (6)

Here, n refers to the total duration of the time series, which in this study spans 38 years (i.e. n = 38).

The two-tailed test employs significance levels of 0.05 (Z = 1.96) and 0.01 (Z = 2.58), representing significant trends at 95 % and 99 % confidence intervals. Consequently, trends in NPP changes across Africa are classified into five categories: extremely significant increase (Sen slope >0 and Z  $\geq$  2.58), extremely significant decrease (Sen slope <0 and Z  $\geq$  2.58), significant increase (Sen slope >0 and 1.96  $\leq$  Z < 2.58),

significant decrease (Sen slope <0 and  $1.96 \le Z < 2.58$ ), and no significant change (Z <1.96).

#### 4.3. Sustainability analysis using Hurst exponent

The Hurst exponent was initially utilized for analyzing flood periodicity and later extensively employed for forecasting future trends in time series, serving as an indicator for differentiating between random walk and biased random walk processes (Tong et al., 2018). This research employs this methodology to assess African NPP and project its forthcoming trends. The fundamental principle is as follows (Gu et al., 2018; Tong et al., 2018; Zhang et al., 2019):

Define the NPP series  $\{NPP(t)\}(t=1,2,\cdots,n)$ , where an average sequence exists for any positive integer  $\tau$ :

$$\langle NPP \rangle_{\tau} = \frac{1}{\tau} \sum_{t=1}^{\tau} NPP(t), (\tau = 1, 2, \dots, n)$$
 (7)

Here,  $\langle NPP \rangle_{\tau}$  is the average sequence of NPP, and NPP(t) is the NPP measurement at a specific observation time. Based on this, the cumulative deviation of  $NPP(t,\tau)$  is determined as:

$$NPP(t,\tau) = \sum_{t=1}^{\tau} (NPP(t) - \langle NPP \rangle_{\tau}), (1 \le t \le \tau)$$
(8)

The sequence  $R(\tau)$  is characterized as follows:

$$R(\tau) = \max_{1 \le t \le \tau} NPP(t, \tau) - \min_{1 \le t \le \tau} NPP(t, \tau), (\tau = 1, 2, \dots, n)$$
(9)

where  $R(\tau)$  is the range of the NPP time series, with  $\max_{1 \leq t \leq \tau} NPP(t,\tau)$  and  $\min_{1 \leq t \leq \tau} NPP(t,\tau)$  denoting the maximum and minimum NPP values, respectively. The sequence of standard deviations, denoted as  $S(\tau)$ , is expressed as:

$$S(\tau) = \left[\frac{1}{\tau} \sum_{t=1}^{\tau} \left(NPP(t) - \langle NPP \rangle_{\tau}\right)^{2}\right]^{\frac{1}{2}}, (\tau = 1, 2, \dots, n)$$
 (10)

R, S,  $\tau$  satisfy the general relationship equation:

$$R(\tau)/S(\tau) = c \cdot \tau^H \tag{11}$$

where c is a constant;  $R(\tau)/S(\tau)$  represents the range of rescaling. The variable H represents the Hurst exponent, and we can obtain its estimated value as:

$$\log(R/S)_{\tau} = \log c + H \cdot \log \tau \tag{12}$$

The H value varies from 0 to 1, each range having a specific interpretation: Values between 0.5 and 1 indicate persistence, where future changes are likely to follow historical trends (e.g., past growth suggests future growth). Persistence is further classified: 0.5 < H < 0.65 indicates weak persistence,  $0.65 \leq H < 0.75$  signifies moderate persistence, and  $0.75 \leq H \leq 1$  signifies strong persistence, with values closer to 1 showing greater persistence. An H value of 0.5 denotes a random walk, implying unpredictable future changes. Values between 0 and 0.5 indicate antipersistence, whereby future trends tend to reverse past trends (e.g., past growth suggests future decline). Anti-persistence is categorized as follows: 0.35 < H < 0.5 indicates weak anti-persistence,  $0.20 \leq H < 0.35$  signifies moderate anti-persistence, and  $0 \leq H < 0.20$  signifies strong anti-persistence, with values closer to 0 showing stronger antipersistence (Zhang et al., 2019).

Following Wang et al. (2023a) and Zhao et al. (2023), we classified criteria for the prospective changes in African NPP (Table 1). Subsequently, we performed a spatial overlay of the Sen's slope trend and the Hurst exponent distribution of African NPP using raster calculations to illustrate these future change characteristics. This illustration was then utilized to evaluate the sustainability of African NPP at the pixel level.

**Table 1**Characteristics of future changes in African NPP based on trend analysis and the Hurst exponent.

Hurst	Theil-Sen slope	Future change characteristics
0–0.5	Increase*	Increase to decrease
	No significant changes	Invariant to variable
	Decrease*	Decrease to increase
0.5–1.0	Increase*	Continuously increase
	No significant changes	Continuously unchanged
	Decrease*	Continuously decrease

Note: \* Includes significant and highly significant levels.

#### 4.4. Structural equation model

The structural equation model (SEM) distinguishes itself from methods such as correlation and regression analysis by its ability to manage multiple driving factors simultaneously (Li et al., 2020). This capability allows for the identification of both direct and indirect impacts (Liu et al., 2022a; Pearl, 2012). Moreover, SEM can elucidate the interrelationships among various factors (Urbach and Ahlemann, 2010). This study employs SEM to investigate the driving forces behind NPP changes in Africa, considering latent variables like climate change, topographic variations, and human activities. Observed variables for climate change include average, maximum, and minimum temperatures, as well as total precipitation. Topographic variables encompass elevation, slope, and aspect, while human activity variables include population density, GDP, and industrial structure. To ensure spatial consistency and data comparability, NPP and all driving factor data were resampled to a  $0.5^{\circ} \times 0.5^{\circ}$  grid, as detailed in Section 2.2.3. Subsequent SEM modeling and analysis were conducted at the pixel scale using the Python platform.

The conceptual SEM in Fig. 2 delineates the factors impacting NPP changes by exploring three hypotheses rooted in geographical knowledge: 1) Direct effects of climate, topography, and human-induced activities on vegetation NPP; 2) Indirect effects of topographic alterations on NPP through climate variations, such as elevation increases leading to temperature decreases affecting vegetation growth; 3) Indirect effects of topographic modifications on NPP through changes in human activities, for instance, restrictions on human activities in high-altitude areas impacting natural resource exploitation.

To identify the most appropriate model, four fit indices were selected for model evaluation: Goodness of Fit Index (GFI), Comparative Fit Index (CFI), Incremental Fit Index (IFI), and Root Mean Square Error of Approximation (RMSEA). A model is considered to fit better when GFI, CFI, and IFI values approach 1, and when RMSEA value approaches 0. Once all fit indices meet the required criteria, the final SEM can be established. By analyzing the standardized path coefficients, the effects (both direct and indirect) of various driving factors can be determined.

This study employs the methods outlined above and the data presented in Section 2.2 to examine the time series characteristics, geographical distribution, historical trends, and future characteristics of African NPP. Additionally, a SEM model is applied to explore the influence mechanisms of both natural and human-induced factors on NPP. The overall research framework is illustrated in Fig. 3.

# 5. Results and analysis

# 5.1. Interannual variation of African NPP

The temporal evolution of African NPP between 1981–2018 is illustrated in Fig. 4. In general, the annual values displayed a fluctuating upward trajectory, rising from 125.1 gC.m $^{-2}$ .a $^{-1}$  in 1981 to 126.9 gC.m $^{-2}$ .a $^{-1}$  in 2018. Over the study period, the slope of NPP change in Africa was 0.3, with an R $^2$  value of 0.35, indicating a highly significant growth trend (P < 0.01). The temporal NPP variation in Africa can be broadly categorized into three phases during the research period, with

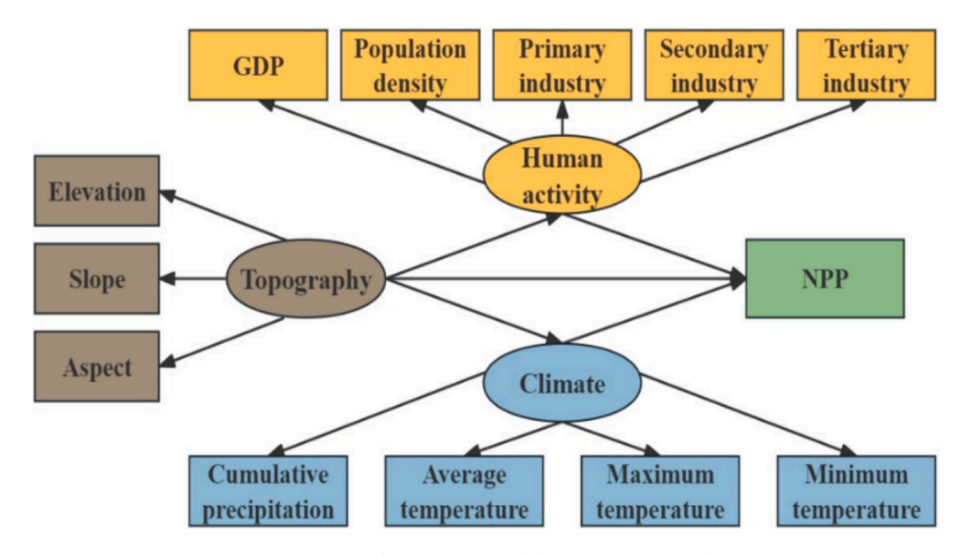


Fig. 2. Conceptual SEM framework for African NPP analysis.

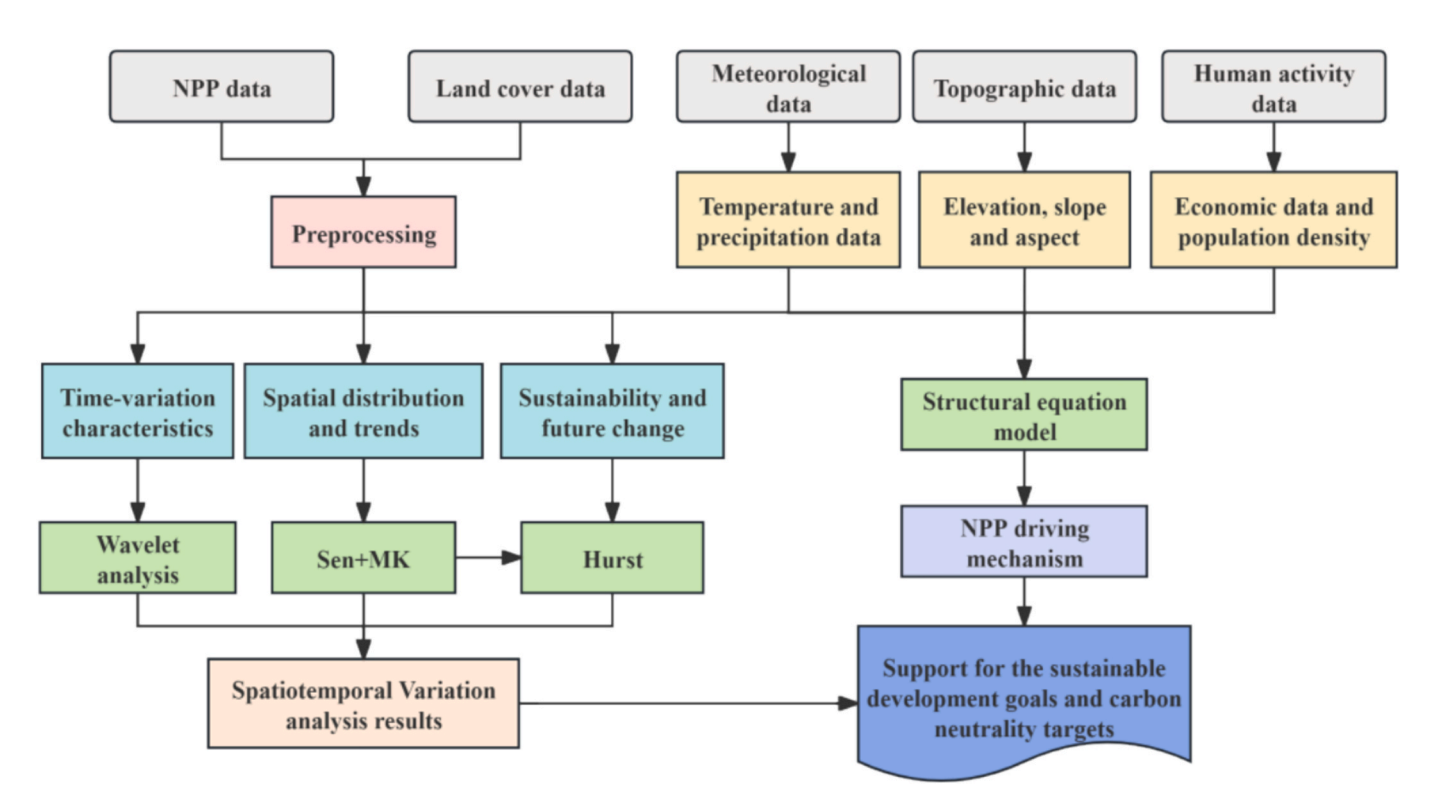


Fig. 3. Analytical workflow for assessing NPP across Africa.

pivotal years in 1992 and 2000. From 1981 to 1992, NPP experienced significant fluctuations, particularly during the period between 1986 and 1992, where NPP declined sharply and reached its lowest point in 1992 (112.3 gC.m $^{-2}$ .a $^{-1}$ ), potentially linked to global cooling and the La Niña phenomenon. Between 1993 and 2000, NPP demonstrated a steady growth pattern, reaching a peak in 2000 (135.2 gC.m $^{-2}$ .a $^{-1}$ ). Post-2001, NPP exhibited a fluctuating decrease, notably between 2014 and 2016, experiencing a marked decline possibly due to prolonged high temperatures and droughts associated with the 2015–2016 El Niño phenomenon in Africa, impacting vegetation growth.

To further analyze the variation patterns of African NPP time series data, Morlet wavelet was used, with the findings presented in Fig. 5. The real part coefficient contour plot (Fig. 5a) indicates that between 1981 and 2018, African NPP exhibited two prominent high points (in 1981).

and 2000) and two low points (in 1992 and 2007), with significant oscillations observed on a time scale of 25–35 years. The wavelet power spectrum (Fig. 5b) demonstrates that after 2000, the NPP series is expected to undergo substantial changes compared to prior years. This result aligns with the interannual analysis of NPP (Fig. 4) and the subsequent sustainability assessment in Section 5.3, which indicates that most regions of Africa are experiencing a trend toward antisustainability. To determine the primary periods of NPP changes accurately, a wavelet variance plot was generated (Fig. 5c), revealing three distinct peaks at time scales of 28, 19, and 7 years. This suggests that the 28-year time scale represents the strongest periodic oscillation in African NPP variation, serving as the primary period, while the 19-year and 7-year time scales represent the secondary and tertiary main periods, respectively. These periodic fluctuations at the three-time scales

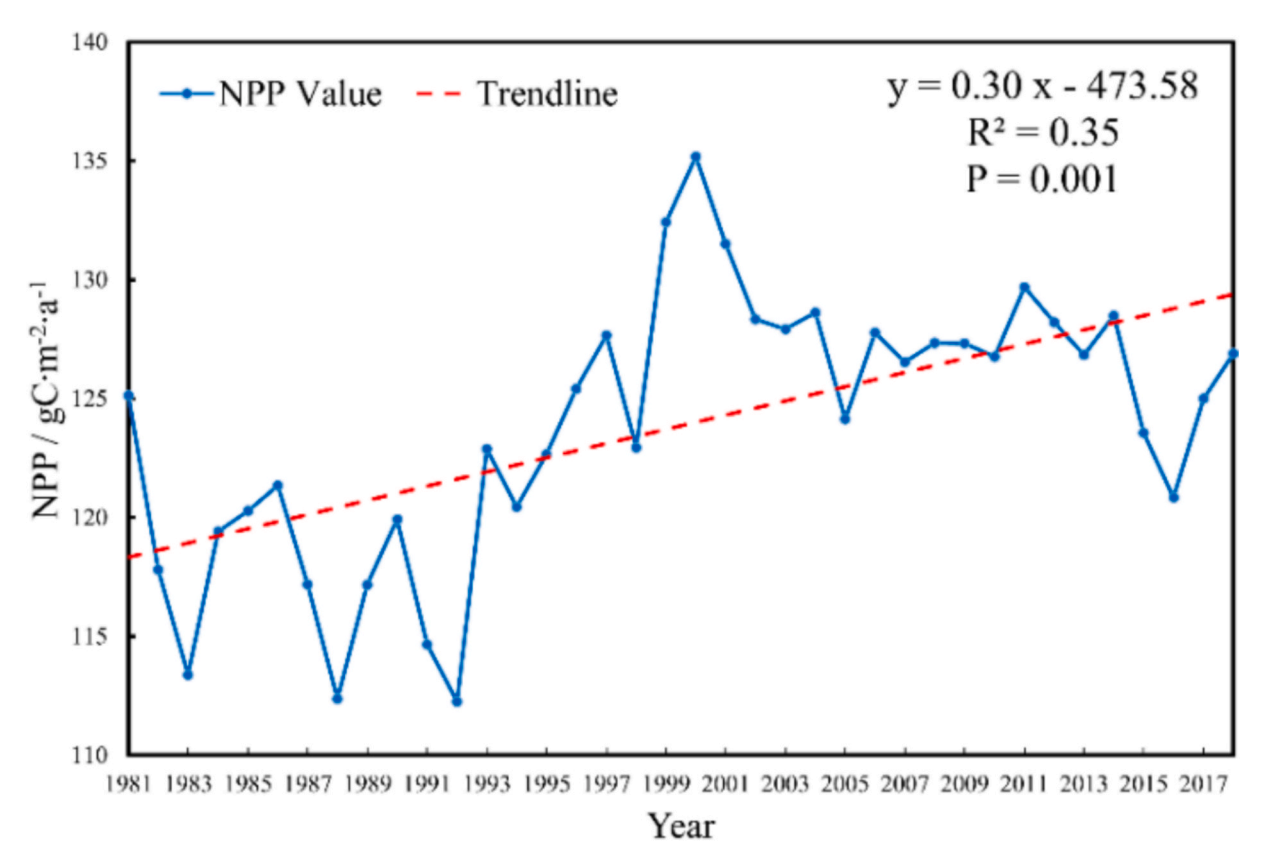


Fig. 4. Interannual variability of NPP in Africa, 1981–2018.

collectively influence the characteristics of NPP variation in Africa throughout the study period. Furthermore, a trend graph of the wavelet primary period under the 28-year time scale (Fig. 5d) illustrated a periodic variation of approximately 20 years in African NPP, with approximately two distinct up-down transition periods observed. These results offer a scientific foundation for understanding the temporal dynamics of African NPP.

# 5.2. Distribution pattern and trend of African NPP

African NPP is predominantly concentrated around the equator, and symmetrically distributed towards the poles. As latitude increases, NPP values gradually decline, and its spatial distribution pattern (Fig. 6) corresponds to the classifications observed in the land cover type map (Fig. 1). Additionally, when considered alongside Africa's precipitation patterns, it can be observed that the dividing lines between areas of extremely high value, high value, median value, and low value of NPP is basically consistent with equivalent rainfall thresholds of 1500 mm, 1000 mm, and 500 mm, respectively. Regions with high NPP values (>290 gC.m<sup>-2</sup>.a<sup>-1</sup>) are primarily situated within the tropical rainforest zone between 5°N and 5°S, extending from the west coast to 30°E. These areas include the Guinea coast, eastern Madagascar, the Congo Basin, Gabon, Liberia, and other equatorial countries, where vegetation thrives year-round, leading to markedly higher NPP relative to other areas. Median NPP areas (150  $\sim 290~\text{ gC.m}^{-2}.\text{a}^{-1}$ ) are primarily located next to tropical rainforest. These regions are dominated by broadleaf, needleleaf, and mixed forests. Low NPP areas (<150 gC.m<sup>-2</sup>.a<sup>-1</sup>) are primarily found in Sahel, eastern East Africa, and southwestern Africa. Notably, NPP in South Africa exhibits a westward decline trend attributable to the southeast trade winds carrying warm water vapor from the coast, which diminishes over the plateau and sinks into the basin, causing a climatic shift from humid in the east to arid in the west.

Fig. 7 presents the spatial trends in NPP across Africa during

1981-2018. Overall, approximately half of Africa (50.8 %) experienced no significant change. Among the regions experiencing significant changes, 40.2 % displayed an upward trend, with 31.1 % exhibiting a highly significant rise. These regions are mainly located in equatorial countries such as Guinea, Ghana, Cameroon, Gabon, and Congo, covering tropical rainforest as well as adjacent coniferous and deciduous forests. The consistent rainy climate in the tropical rainforest, coupled with global warming, has led to enhanced vegetation productivity due to adequate rainfall. However, there are still small areas (9 %) exhibiting a decreasing trend, with 5.5 % demonstrating a highly significant decline, primarily located in grasslands, croplands, and shrub cover regions north of the tropical rainforest. Notably, despite broadly similar landcover types south and north of the rainforest, the NPP trends vary, potentially due to topographical differences. Additionally, certain localized areas within the tropical rainforest region (e.g., border regions between the Kellet Mountains and the Congo Basin) indicate a highly significant decrease in NPP, primarily attributed to human logging activities.

# 5.3. Sustainability assessment of African NPP

To assess the sustainability of vegetation dynamics in Africa, the Hurst exponent of NPP was calculated (Fig. 8). The analysis revealed that a substantial portion of Africa (72.3 %) demonstrated an H value < 0.5, with a mean value of 0.424, reflecting a general trend of antisustainability in NPP. This result aligns with the findings in Section 5.1, where wavelet analysis showed a substantial change in the NPP sequence after 2000 compared to earlier periods. This suggests a potential reversal in the increasing pattern of African NPP over the forthcoming period. Notably, regions demonstrating strong antisustainability constitute 44.9 % of the area, predominantly concentrated in tropical rainforests, deciduous broadleaf forests, and deciduous needleleaf forests. This indicates that despite the upward trend observed

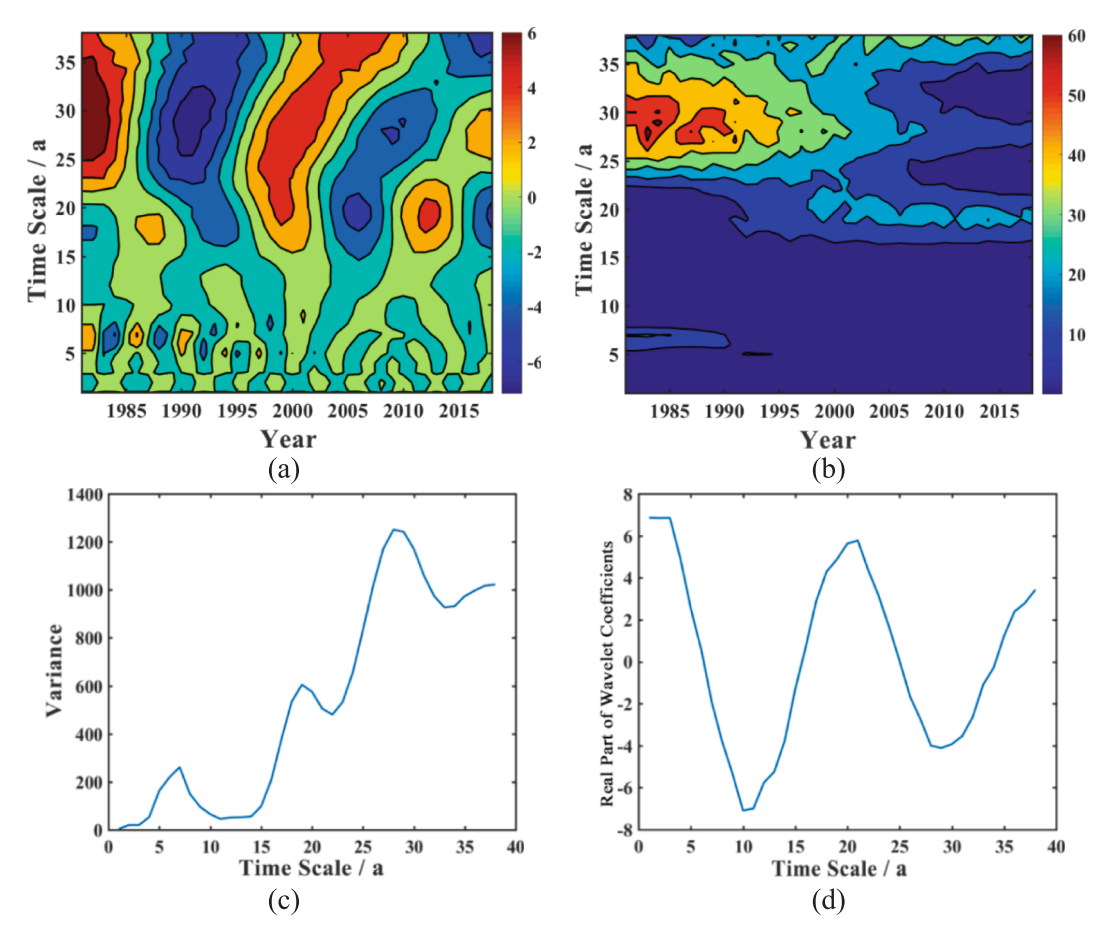


Fig. 5. Wavelet analysis of temporal variability in African NPP (1981–2018): (a) real-part wavelet coefficient contours; (b) wavelet power spectrum; (c) wavelet variance; (d) temporal evolution of the dominant period.

in regions with high NPP such as the African tropical rainforests over the study period, NPP might undergo significant fluctuations due to global warming and intensified drought conditions. Conversely, regions with H values >0.5 are sparse and fragmented, encompassing only 15.7 % of the total area, mainly comprising grasslands, croplands, and shrublands. Among these, wetlands within tropical rainforests display strong sustainability, likely attributed to their unique natural environment characteristics that enable effective regulation of drought and other environmental stressors, thereby maintaining local ecosystem balance and stability.

A comprehensive visualization of the future changes in African NPP is produced by examining the Hurst exponent calculations of the African NPP (Fig. 8) alongside the trend analysis result (Fig. 7). This figure (Fig. 9) provides a clearer representation of the anticipated NPP variations across Africa. The analysis reveals that a mere 10.4 % of the African region is projected to sustain an upward trend in NPP, including wetlands that exhibit significant resilience against drought and other calamities. However, a predominant portion of the area (52.8 %) is expected to shift from an increasing to a decreasing NPP trend, which includes most tropical rainforests, deciduous broadleaf forests, and deciduous needleleaf forests. Additionally, 4.4 % of the regions are predicted to continue in a declining NPP trend, while 19 % of the areas are projected to shift from a decreasing trend to an increasing one. It is noteworthy that regions persisting in decline and those shifting towards an increase are relatively fragmented and dispersed. These areas are mainly located in Ethiopia, central Kenya, Somalia, southern Sudan and Chad, the Central African Republic, southern Niger, Nigeria, and Ghana-regions heavily impacted by anthropogenic activities. In these countries, certain regions remain affected by human activities, notably deforestation driven by agricultural and livestock expansion, resulting

in a continuous decline in NPP. Conversely, the implementation of ecological projects like reforestation has progressively restored the ecological environment in some regions, reversing the trend from a previous decline or negligible change to an increase.

# 5.4. Driving mechanisms of NPP in Africa

This study employs SEM to evaluate the effects of natural factors (precipitation, temperature, and topography) and human-induced factors (population density, GDP, and economic structure) on NPP in Africa. Among the various factors analyzed, only the impact of the primary industry failed to meet the threshold for significance, while the effects of the other factors are illustrated in Fig. 10. The model's goodness-of-fit indices—GFI, CFI, and IFI—are 0.977, 0.894, and 0.895, respectively, with an RMSEA below 0.15, indicating satisfactory fit and reliability.

The results indicate climate has a predominantly direct effect on NPP variations across Africa, with a significant impact coefficient of 0.89. Cumulative precipitation is the primary determinant of climate change's impact on NPP (impact coefficient of 0.85), followed by maximum and minimum temperatures (impact coefficients of -0.63 and 0.52, respectively). The mean temperature's contribution is relatively minor, with an impact coefficient of merely 0.03. Human activities also directly affect NPP variations, albeit to a lesser extent than climate factors, with an impact coefficient of 0.05. The analysis further reveals that GDP is the primary human activity influencing NPP (impact coefficient of 0.3). In contrast, the contributions of population density and industrial structure are minimal (impact coefficient for population density is 0.07; primary industry impact is below the model's minimum analysis threshold, while the impact coefficients for secondary and tertiary industries are both 0.08).

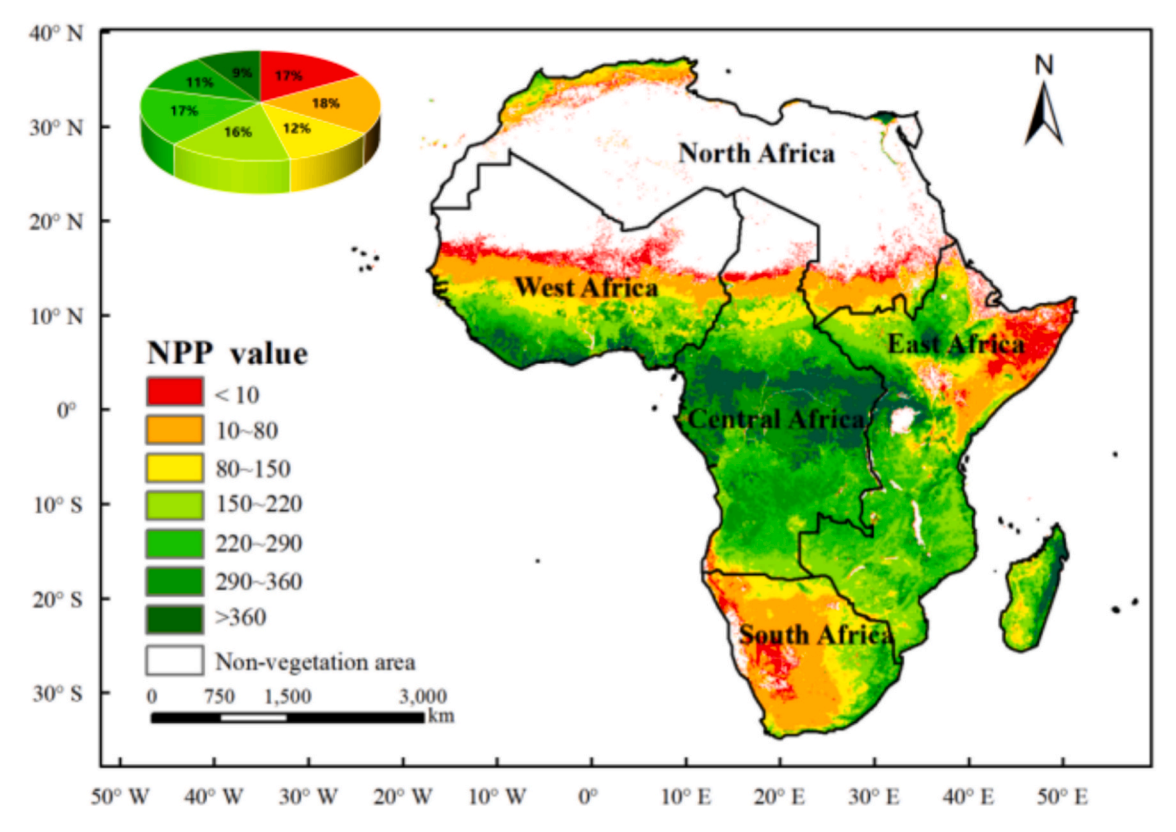


Fig. 6. Spatial distribution of mean NPP across Africa, 1981-2018.

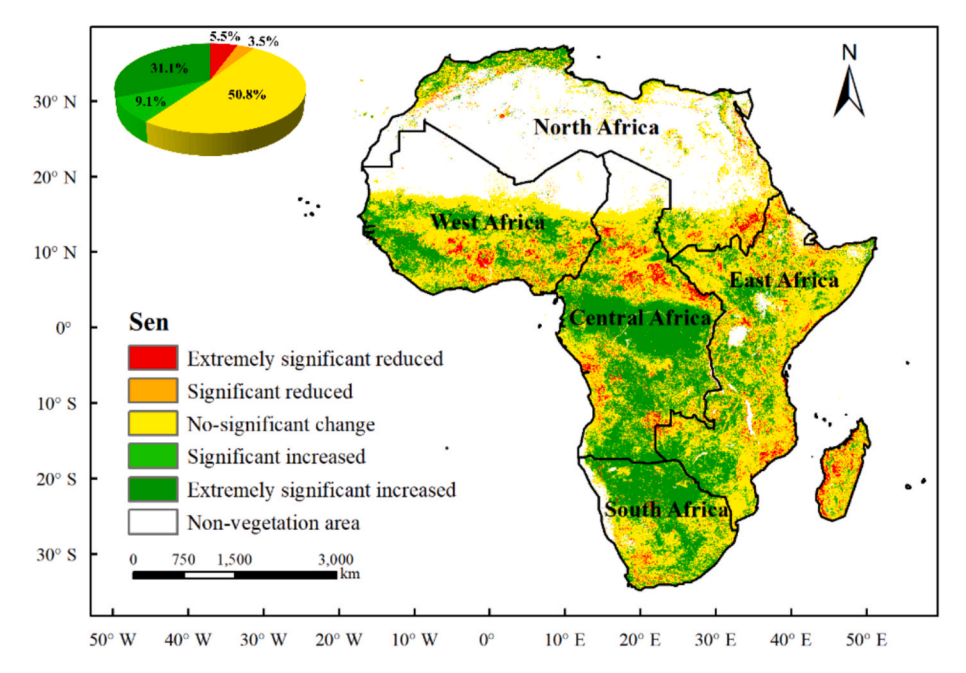


Fig. 7. Spatial pattern of NPP trend characteristics across Africa, 1981-2018.

The influence of topography on NPP is multifaceted, encompassing both direct and indirect effects. The direct impact of topography on NPP is minor, as indicated by a coefficient of 0.04. Among topographic factors, slope variation most accurately represents topography's impact on NPP, with a coefficient of 0.73, whereas aspect has a negative impact coefficient of -0.39, and elevation's contribution is minimal (coefficient of 0.04). Furthermore, topography influences NPP through its effects on climate and human activities, with impact coefficients of approximately

0.01 (derived as  $0.2\times0.05$ , i.e., the coefficient between topography and human activities multiplied by that between human activities and NPP) and 0.61 (derived as  $0.68\times0.89$ , i.e., the coefficient between topography and climate multiplied by that between climate and NPP), respectively. When considering both direct and indirect influences, the cumulative coefficient for topography is around 0.66. This indicates that although the direct impact of topography is relatively minor, its indirect influence via climate significantly amplifies the overall effect.

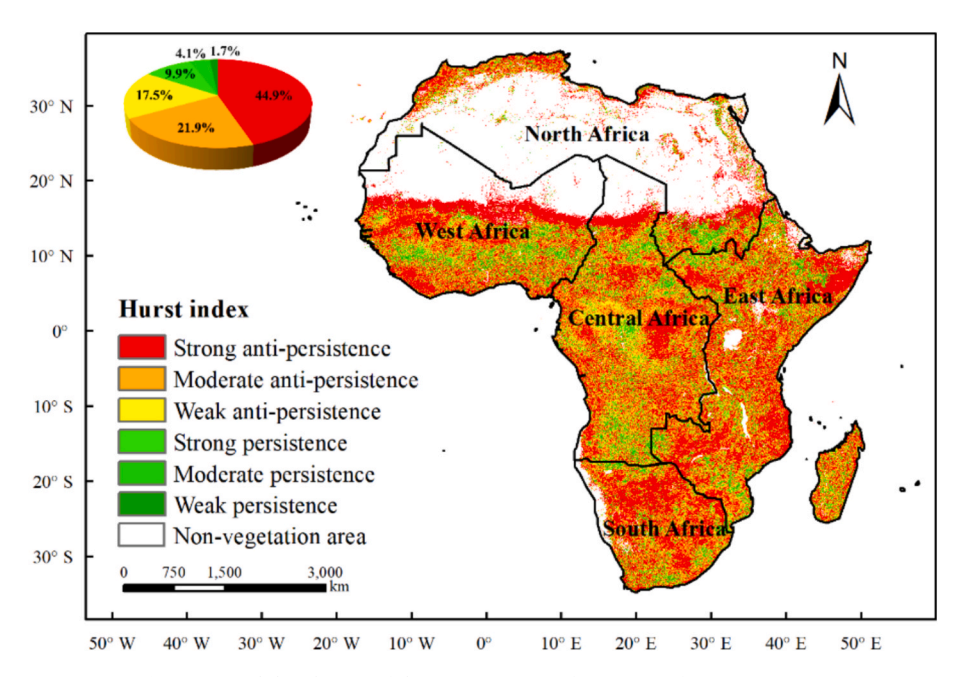


Fig. 8. Spatial distribution of the Hurst exponent for NPP in Africa, 1981-2018.

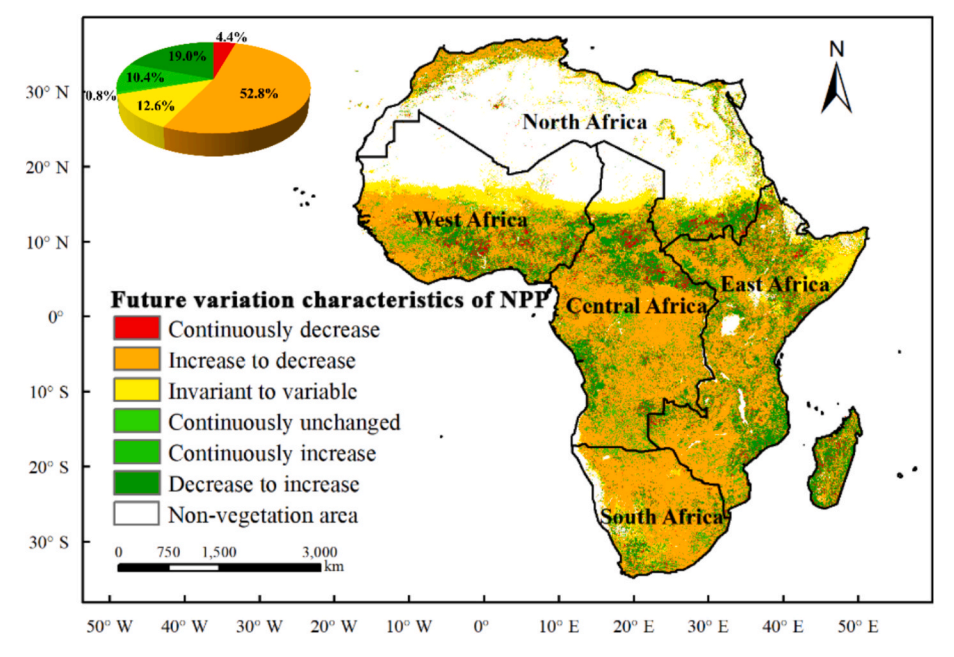


Fig. 9. Characteristics of future NPP changes across Africa.

Among the driving factors, climate change emerges as the most influential, with a coefficient of 0.89. Topography follows with a coefficient of 0.66, while human activities exert the least influence, with an impact coefficient of 0.05.

#### 6. Discussion

# 6.1. Spatiotemporal variability of NPP in Africa

Temporally, African NPP exhibited a generally increasing but highly variable trajectory from 1981 to 2018. This timeframe can be divided into three distinct phases, demarcated by the years 1992 and 2000: an era of severe fluctuations from 1981 to 1992, a period of stable growth from 1993 to 2000, and an era of fluctuating decline post-2001.

Concurrently, Africa's hydrothermal conditions underwent analogous changes. Temperature trends exhibited a "decline – rise – stabilization" pattern, while precipitation trends followed a "decline – rise – decline – stabilization" sequence (Ferchichi et al., 2024; Shi et al., 2023). These observations imply that variations in NPP were predominantly driven by hydrothermal conditions, corroborating the analysis presented in section 5.2.

Geographically, the highest NPP values in Africa are observed in the central region of Central Africa, followed by the southern region of West Africa. In contrast, the lowest NPP values are located north of  $15^\circ$  latitude and in South Africa. This spatial distribution is closely linked to land cover types. The central region of Central Africa is predominantly covered by tropical rainforests, whereas areas north of  $15^\circ$  latitude and in South Africa encompass the vast Saharan desert and the arid regions

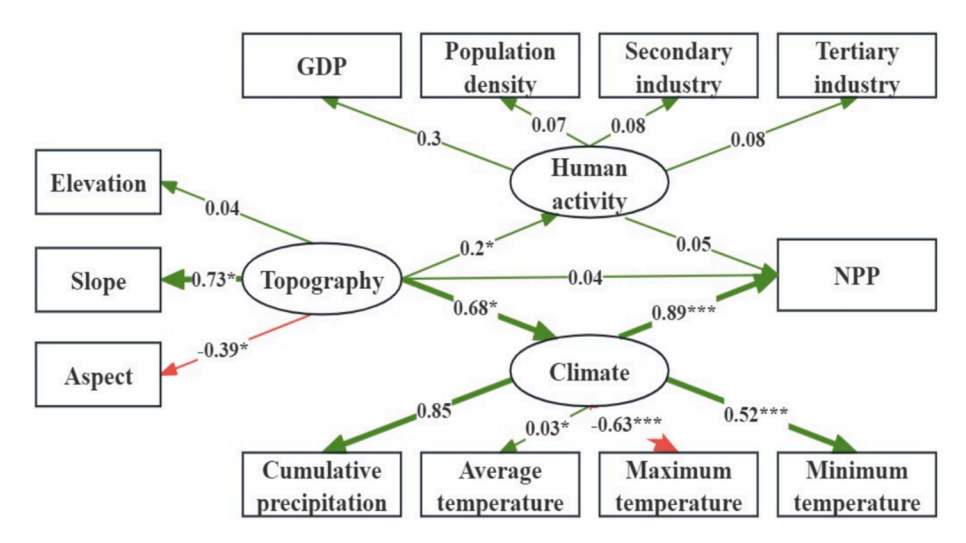


Fig. 10. SEM path diagram quantifying drivers of NPP variability in Africa. Note: \*\*\* p < 0.01; \*\* p < 0.05; \* p < 0.10.

of South Africa, respectively. Overall, NPP is significantly influenced by ecosystem type, with productivity ranking from highest to lowest as follows: tropical rainforest > deciduous forest > shrubland > cropland > grassland > desert. These results align with the work of Wang et al. (2023b) and Shi et al. (2023).

#### 6.2. Trends and sustainability of NPP in Africa

Driven by factors such as global warming, the NPP in Africa is generally increasing, reflecting global climatic patterns and corroborating the findings of Piao et al. (2020). Nonetheless, NPP changes across the continent show spatial variability.

Tropical rainforests near the equator, which benefit from consistent rainfall and stable precipitation without distinct dry and wet seasons, typically exhibit a significant upward trend in undisturbed areas and adjacent vegetation under global warming. Conversely, regions such as East Africa, the northern part of Central Africa, and areas near the Sahara Desert display a notable downward trend.

This is primarily due to two reasons. First, African climate is marked by extreme weather patterns, with frequent droughts and floods directly impacting plant growth (Ferchichi et al., 2024; Shi et al., 2023). In contrast, temperate regions, although affected by climate change, have relatively stable NPP due to better ecosystem adaptability (Liang et al., 2022; Piao et al., 2020; Reichstein et al., 2013). Second, human activities such as destructive agricultural practices and overgrazing have driven severe deforestation. Over the past thirty years, Africa has lost more than 15 % of its forest cover, making it the most deforested region globally, with approximately 4 million hectares of forest cut or burned annually—an area roughly twice the size of Rwanda (Wang and Wang, 2015). This deforestation has destabilized ecosystems, leading to decreased NPP. In other continents, particularly North America, Europe and Asia, despite land use changes, the adoption of sustainable agricultural and forest management practices has allowed agricultural and pastoral lands to maintain or even increase NPP (Chen et al., 2019; Gelfand et al., 2013).

Furthermore, analysis using the Hurst exponent reveals that NPP in most African regions exhibits strong anti-sustainable changes, primarily due to the significant impact of climatic factors on NPP. In areas unaffected by natural disasters or human activities, global warming has generally promoted plant NPP growth. However, Africa's already high average temperatures mean that further warming often leads to extreme heat and drought, causing ecological disruptions (Ferchichi et al., 2024; Shi et al., 2023). These factors, combined with detrimental human activities such as deforestation, result in anti-sustainable trends in NPP across much of Africa (Antropov et al., 2021; Reichstein et al., 2013;

# Richard et al., 2016).

To tackle these challenges, it is crucial to adopt human intervention strategies, including soil and water conservation and ecological restoration, to cope with extreme climate conditions in Africa, prevent natural disasters from damaging ecosystems, and enhance ecosystem resilience. Additionally, sustainable management measures in agriculture and animal husbandry are needed to optimize land use planning, improve land productivity and ecological benefits, reduce over-reliance on ecological resources, and protect and restore ecosystem stability.

# 6.3. Drivers of NPP variability in Africa

Vegetation NPP is governed by multiple drivers, which may act independently or synergistically. Prior research has emphasized the direct effects of topography on NPP (Peng et al., 2019). However, topographic variables also modulate temperature, hydrothermal conditions, and human activities to varying extents, thereby exerting an indirect influence on NPP fluctuations. Findings reveal that considering only the direct influence of topography on NPP yields a minimal impact, with an influence coefficient of just 0.04, the lowest among all factors examined. Conversely, when accounting for topography's indirect effects through its modulation of climate, the cumulative influence coefficient escalates to 0.66. This value is second only to the influence of climatic factors (0.89) and significantly higher than the effect of human activities (0.05). Consequently, reliance on simplistic approaches like correlation analysis may lead to an underestimate of topography's overall impact on NPP. Thus, the application of comprehensive methodologies such as SEM, which can capture the intricate interrelations among various factors, is imperative for the precise evaluation of their impacts on NPP.

Hydrothermal conditions are pivotal determinants of NPP (Yang et al., 2024). The Saharan and South African arid regions rank among the world's eight most arid zones, with extreme dryness and annual precipitation between 50 and 100 mm (Ferchichi et al., 2024; Shi et al., 2023). In these areas, water scarcity significantly limits plant growth. This study shows that among climatic variables impacting NPP, cumulative precipitation has the most substantial effect, with an impact coefficient of 0.85. Additionally, the analysis indicates that average temperature has a minimal effect, with a coefficient of only 0.03. In contrast, an increase in minimum temperature significantly boosts NPP, with an impact coefficient of 0.52, whereas maximum temperature negatively affects NPP, as indicated by an impact coefficient of -0.6. The analysis presented in Section 5.2 reveals that a significant portion of Africa (40.2 %) shows an upward trend in vegetation NPP, suggesting that under global warming conditions, Africa, often called the "tropical

continent," is experiencing increased NPP, which supports Wang et al. (2023b). The underlying cause of this phenomenon is the rise in minimum temperatures. Given Africa's already high average temperatures, further increases have a negligible impact on NPP enhancement. However, rising minimum temperatures can still promote vegetation growth, contributing to the observed NPP increase. Conversely, if maximum temperatures continue to rise, there is a higher risk of extreme heat events, which can accelerate soil moisture evaporation, leading to severe droughts. Such conditions can adversely affect vegetation growth. Consequently, our analysis indicates that in Africa, maximum air temperature is negatively correlated with NPP.

Human activities exhibit a dual influence on NPP (Liu et al., 2021a, d). Unsustainable agricultural practices and urban sprawl contribute to the deterioration of vegetation, whereas ecological conservation projects can promote its growth (He et al., 2021). Our analysis reveals that in Africa, human activities have a relatively minor effect, with GDP being the primary determinant. There is little correlation observed with population density and industrial structure. This is due to Africa's vast land area and low population density relative to its large population, resulting in limited human impact, particularly in remote and uninhabitable regions where NPP variations are mainly driven by natural factors. Additionally, economically advanced African nations such as Ethiopia, Kenya, and Nigeria have implemented measures like establishing nature reserves and curbing illegal logging to reduce the adverse impacts of agricultural and pastoral development on vegetation. These ecological engineering interventions have facilitated vegetation restoration, partially counterbalancing the negative impacts of human activities. As a result, there is a weak positive correlation between socioeconomic factors and NPP, as evidenced by a coefficient value of 0.3.

The above analysis indicates that, besides precipitation, the highest and lowest temperatures are also key factors affecting African NPP. The increase in minimum temperature promotes NPP, while the rise in maximum temperature negatively impacts it. Therefore, in the context of global warming, Africa's NPP may benefit from increasing minimum temperatures but also faces the threat of extreme heat and drought events caused by rising maximum temperatures. To address this challenge, effective human intervention measures such as enhancing soil moisture retention, promoting drought-tolerant crop varieties, and undertaking ecological restoration projects should be implemented. These measures are crucial for improving ecosystem resilience and reducing the impact of high temperatures on ecosystems, which is vital for sustainable development in Africa.

# 6.4. Limitations and future prospects

While the SEM model is effective in evaluating the contributions of various factors to NPP and elucidating their interactions, its construction is inherently dependent on the selected variables (Li et al., 2020; Liu et al., 2022a). This dependency may result in the omission of potential influencing factors. For instance, this study employs SEM to analyze the driving effects of nature and human factors. However, the absence of comprehensive data has resulted in the exclusion of factors such as natural disasters and deforestation. Future studies will improve the model's comprehensiveness and accuracy by incorporating additional variables, such as soil properties, biodiversity, natural disasters, deforestation, and the fertilization effect of increased  $\rm CO_2$  concentration (Piao et al., 2020; Wang et al., 2020).

Additionally, this research primarily addresses the overall and regional characteristics of NPP changes across the African continent, lacking a detailed analysis of NPP changes and their driving mechanisms within specific ecosystems or vegetation types (e.g., grasslands, deserts, wetlands). Moreover, uncertainties in the NPP datasets—including assumptions of remote sensing inversion models, limitations in spatial resolution, and temporal discrepancies among multi-source sensors—may introduce errors during the analysis process. Future work

should integrate multi-source remote sensing data products and conduct detailed studies on typical ecosystems to strengthen the reliability of conclusions regarding NPP changes and deepen the understanding of their underlying mechanisms.

#### 7. Conclusions

In this paper, the spatiotemporal variations of NPP across Africa during 1981–2018, as well as its driving mechanisms, were analyzed using a long-term NPP dataset. The main conclusions are as follows:

- (1) In the study period, the annual variations of African vegetation NPP demonstrated a fluctuating upward trajectory (P=0.001). This trend can be characterized by three distinct phases: a period of marked fluctuations from 1981 to 1992, a phase of consistent growth from 1993 to 2000, and a subsequent phase of fluctuating decline post-2001. Wavelet analysis revealed that the years 1981 and 2000 were high centers of NPP, while 1992 and 2007 were identified as low centers. Over a 28-year timescale, NPP exhibited a cyclic fluctuation of approximately 20 years with two rise and fall transitions during the study period.
- (2) Spatially, African NPP declines approximately symmetrically from the equator toward higher latitudes. High NPP values are concentrated in the tropical rainforest zone between 5°N and 5°S, while medium values are located in surrounding areas of deciduous broadleaf, needleleaf, and mixed forest regions. Low values are observed in the northern Sahel, eastern East Africa, and southwestern Africa. Trend analysis shows a significant increase in tropical rainforests and adjacent areas, covering 40.2 % of Africa's land area. Conversely, regions like the Congo Basin, Ghana, and Gabon have experienced a significant decline in NPP due to human activities, affecting 9 % of the total area. Hurst exponent analysis suggests a general anti-sustainability trend within Africa's NPP, indicating that 52.8 % of regions may shift from growth to decline in the future, raising concerns about the sustainability of African vegetation.
- (3) The SEM model analysis indicates that NPP variations in Africa are predominantly driven by natural factors, with climate being the most critical factor, exhibiting an impact coefficient of 0.89, primarily regulated by cumulative precipitation and temperature extremes. Topographic factors have a total impact coefficient of 0.66, largely affecting NPP indirectly through climate influence, with a direct impact of only 0.04. Human activities exert a minimal influence on NPP, with an impact coefficient of just 0.05, and GDP changes can effectively measure their effect on NPP variations.

# CRediT authorship contribution statement

Liang Liang: Writing – review & editing, Writing – original draft, Supervision, Project administration, Methodology, Investigation, Funding acquisition, Data curation, Conceptualization. Meng Li: Writing – review & editing, Visualization, Formal analysis. Ziru Huang: Writing – review & editing, Visualization, Validation, Investigation. Qianjie Wang: Writing – original draft, Validation, Data curation. Zhen Yang: Writing – review & editing, Visualization, Software, Resources. Shuguo Wang: Writing – review & editing, Validation, Resources, Methodology.

# Declaration of competing interest

The authors declare that they have no known competing financial interests or personal relationships that could have appeared to influence the work reported in this paper.

#### Acknowledgment

This study was supported by the National Natural Science Foundation of China (No. 42371322), the Fundamental Research Project of Xuzhou (No. KC23079), and the "343" Industrial Development Project of Xuzhou (No. gx2024012).

#### Data availability

Data will be made available on request.

#### References

- Antropov, O., Rauste, Y., Praks, J., Seifert, F.M., Häme, T., 2021. Mapping Forest Disturbance due to Selective Logging in the Congo Basin with RADARSAT-2 Time Series. Remote Sens. 13, 740. https://doi.org/10.3390/rs13040740.
- Brandt, M., Rasmussen, K., Peñuelas, J., Tian, F., Schurgers, G., Verger, A., Mertz, O., Palmer, J.R.B., Fensholt, R., 2017. Human population growth offsets climate-driven increase in woody vegetation in sub-Saharan Africa. Nat. Ecol. Evol. 1, 0081. https://doi.org/10.1038/s41559-017-0081.
- Berdugo, M., DelgadoBaquerizo, M., Soliveres, S., HernándezClemente, R., Zhao, Y., Gaitán, J.J., Gross, N., Saiz, H., Maire, V., Lehmann, A., Rillig, M.C., Solé, R.V., Maestre, F.T., 2020. Global ecosystem thresholds driven by aridity. Science 367, 787–790. https://doi.org/10.1126/science.aay5958.
- Chen, C., Park, T., Wang, X., Piao, S., Xu, B., Chaturvedi, R.K., Fuchs, R., Brovkin, V., Ciais, P., Fensholt, R., Tømmervik, H., Bala, G., Zhu, Z., Nemani, R.R., Myneni, R.B., 2019. China and India lead in greening of the world through land-use management. Nat. Sustain. 2, 122–129. https://doi.org/10.1038/s41893-019-0220-7.
- Chen, J., Shao, Z., Huang, X., Hu, B., 2024. Multi-source data-driven estimation of urban net primary productivity: a case study of Wuhan. Int. J. Appl. Earth Obs. Geoinf. 127, 103638. https://doi.org/10.1016/j.jag.2023.103638.
- Chen, J., Chen, J., Liao, A., Cao, X., Chen, L., Chen, X., He, C., Han, G., Peng, S., Lu, M., Zhang, W., Tong, X., Mills, J., 2015. Global land cover mapping at 30m resolution: a POK-based operational approach. ISPRS J. Photogramm. Remote Sens. 103, 7–27. https://doi.org/10.1016/j.isprsjprs.2014.09.002.
- Espoir, D.K., Sunge, R., Nchofoung, T., Alola, A.A., 2024. Analysing the drivers of ecological footprint in Africa with machine learning algorithm. Environ. Impact Assess. 104, 107332. https://doi.org/10.1016/j.eiar.2023.107332.
- Ferchichi, A., Chihaoui, M., Ferchichi, A., 2024. Spatio-temporal modeling of climate change impacts on drought forecast using Generative Adversarial Network: a case study in Africa. Expert Syst. Appl. 238, 122211. https://doi.org/10.1016/j. eswa.2023.122211.
- Field, C.B., Behrenfeld, M.J., Randerson, J.T., Falkowski, P., 1998. Primary production of the biosphere: integrating terrestrial and oceanic components. Science 281, 237–240. https://doi.org/10.1126/science.281.5374.237.
- Gelfand, I., Sahajpal, R., Zhang, X., Izaurralde, R.C., Gross, K.L., Robertson, G.P., 2013. Sustainable bioenergy production from marginal lands in the US Midwest. Nature 493, 514–517. https://doi.org/10.1038/nature11811.
- Ghaderpour, E., Mazzanti, P., Mugnozza, G.S., Bozzano, F., 2023. Coherency and phase delay analyses between land cover and climate across Italy via the least-squares wavelet software. Int J Appl Earth Obs. 118, 103241. https://doi.org/10.1016/j. iov.2023.103241.
- Gocic, M., Trajkovic, S., 2013. Analysis of changes in meteorological variables using Mann-Kendall and Sen's slope estimator statistical tests in Serbia. Glob. Planet. Change. 100, 172–182. https://doi.org/10.1016/j.gloplacha.2012.10.014.
- Gong, P., Liu, H., Zhang, M., Li, C., Wang, J., Huang, H., Clinton, N., Ji, L., Li, W., Bai, Y., Chen, B., Xu, B., Zhu, Z., Yuan, C., Suen, H.P., Guo, J., Xu, N., Li, W., Zhao, Y., Yang, J., Yu, C., Wang, X., Fu, H., Yu, L., Dronova, I., Hui, F., Cheng, X., Shi, X., Xiao, F., Liu, Q., Song, L., 2019. Stable classification with limited sample: transferring a 30-m resolution sample set collected in 2015 to mapping 10-m resolution global land cover in 2017. Sci. Bull. 64, 370–373. https://doi.org/10.1016/j.scib.2019.03.002.
- Gu, Z., Duan, X., Shi, Y., Li, Y., Pan, X., 2018. Spatiotemporal variation in vegetation coverage and its response to climatic factors in the Red River Basin. China. Ecol. Indic. 93, 54–64. https://doi.org/10.1016/j.ecolind.2018.04.033.
- Güçlü, Y.S., 2020. Improved visualization for trend analysis by comparing with classical Mann-Kendall test and ITA. J. Hydrol. 584, 124674. https://doi.org/10.1016/j. ihydrol.2020.124674.
- He, X., Yu, Y., Cui, Z., He, T., 2021. Climate Change and Ecological Projects Jointly Promote Vegetation Restoration in Three-River Source Region of China. Chin. Geogr. Sci. 31 (6), 1108–1122. https://doi.org/10.1007/s11769-021-1245-1.
- Hutley, L.B., Beringer, J., Fatichi, S., Schymanski, S.J., Northwood, M., 2022. Gross primary productivity and water use efficiency are increasing in a high rainfall tropical savanna. Glob. Chang. Biol. 28, 2360–2380. https://doi.org/10.1111/ gcb.16012.
- Igboeli, E.E., Chukwuka, O., Ochege, F.U., Onyekwelu, C.A., Ling, Q., Ajaero, C., Hamdi, R., Rahman, M., Kayiranga, A., Luo, G., 2025. Combined impacts of land change and climate variability on ecosystem net primary productivity in arid regions. Glob. Planet. Change. 245, 104682. https://doi.org/10.1016/j. gloplacha.2024.104682.

- Jin, Y., Lin, Q.N., Mao, S.P., 2022. Challenges and Countermeasures for Deepening China-Africa Agricultural Investment Cooperation. Intertrade 10, 19–26. https://doi. org/10.14114/j.cnki.itrade.2022.10.009.
- Li, Z., Han, X., Lin, X., Lu, X., 2020. Quantitative analysis of landscape efficacy based on structural equation modelling: Empirical evidence from new chinese style commercial streets. Alex. Eng. J. 60, 261–271. https://doi.org/10.1016/j. 201.08.005
- Liang, L., Wang, Q., Qiu, S., Chen, B., Wang, S., Geng, D., Wu, J., 2023. NEP Estimation of Terrestrial Ecosystems in China using an improved CASA Model and Soil Respiration Model. IEEE JSTARS. 16, 10203–10215. https://doi.org/10.1109/ ISTARS.2023.3325774
- Liang, L., Geng, D., Yan, J., Qiu, S., Shi, Y., Wang, S., Wang, L., Zhang, L., Kang, J., 2022. Remote Sensing Estimation and Spatiotemporal Pattern Analysis of Terrestrial Net Ecosystem Productivity in China. Remote Sens. 14, 1902. https://doi.org/10.3390/ rs14081902.
- Liu, C., Li, W., Wang, W., Zhou, H., Liang, T., Hou, F., Xu, J., Xue, P., 2021a. Quantitative spatial analysis of vegetation dynamics and potential driving factors in a typical alpine region on the northeastern Tibetan Plateau using the Google Earth Engine. Catena 206, 105500. https://doi.org/10.1016/j.catena.2021.105500.
- Liu, C., Zhang, F., Wang, X., Chan, N.W., Rahman, H.A., Yang, S., Tan, M.L., 2022a. Assessing the factors influencing water quality using environment water quality index and partial least squares structural equation model in the Ebinur Lake Watershed, Xinjiang. China. Environ. Sci. Pollut. Res. 29 (8), 1–16. https://doi.org/ 10.1007/s11356-021-17886-5.
- Liu, L., Sun, R., Bai, Y., Niu, Z., 2021b. Stereo Observation and Inversion of the Key Parameters of Global Carbon Cycle:Project Overview and Mid-Term Progresses. Remote Sens. Technol. Appl. 36, 11–24. https://doi.org/10.11873/j.issn.1004-0323.2021.1.0011.
- Liu, Q., Liu, L., Zhang, Y., Wang, Z., Wu, J., Li, L., Li, S., Paudel, B., 2021d. Identification of impact factors for differentiated patterns of NDVI change in the headwater source region of Brahmaputra and Indus. Southwestern Tibetan Plateau. Ecol. Indic. 125, 107604. https://doi.org/10.1016/j.ecolind.2021.107604.
- Mao, R., Xing, L., Wu, Q., Song, J., Li, Q., Long, Y., Shi, Y., Huang, P., Zhang, Q., 2024. Evaluating net primary productivity dynamics and their response to land-use change in the loess plateau after the "grain for Green" program. J. Environ. Manage. 360, 12112. https://doi.org/10.1016/j.jenyman.2024.121112.
- Maluleke, A., Feig, G., Brümmer, C., Jaars, K., Hamilton, T., Midgley, G., 2025. Paired eddy covariance site reveals consistent net C sinks over three growing seasons in an african arid and grassy shrubland. Agric. For. Meteorol. 372, 110705. https://doi. org/10.1016/j.agrformet.2025.110705.
- Nicholson, S.E., 2017. Climate and climatic variability of rainfall over eastern Africa. Rev. Geophys. 55, 590–635. https://doi.org/10.1002/2016RG000544.
- Pearl, J., 2012. The causal mediation formula—a guide to the assessment of pathways and mechanisms. Prev. Sci. 13 (4), 426–436. https://doi.org/10.1007/s11121-011-0270-1.
- Peng, W., Kuang, T., Tao, S., 2019. Quantifying influences of natural factors on vegetation NDVI changes based on geographical detector in Sichuan, western China. J. Clean. Prod. 233, 353–367. https://doi.org/10.1016/j.jclepro.2019.05.355.
- Piao, S., Wang, X., Park, T., 2020. Characteristics, drivers and feedbacks of global greening. Nat. Rev. Earth Environ. 1, 14–27. https://doi.org/10.1038/s43017-019-0001-x.
- Reichstein, M., Bahn, M., Ciais, P., Frank, D., Mahecha, M.D., Seneviratne, S.I., Zscheischler, J., Beer, C., Buchmann, N., Frank, D.C., Papale, D., Rammig, A., Smith, P., Thonicke, K., van der Velde, M., Vicca, S., Walz, A., Wattenbach, M., 2013. Climate extremes and the carbon cycle. Nature 500, 287–295. https://doi.org/ 10.1038/nature12350.
- Richard, S.K., Sonwa, D., Atyi, R., Nkal, N., 2016. Quantifying post logging biomass loss using satellite images and ground measurements in Southeast Cameroon. J. For. Res. 27, 1415–1426. https://doi.org/10.1007/s11676-016-0277-3.
- Shi, S., Yang, P., van der Tol, C., 2023. Spatial-temporal dynamics of land surface phenology over Africa for the period of 1982–2015. Heliyon 9, e16413. https://doi. org/10.1016/j.heliyon.2023.e16413.
- Tong, S., Zhang, J., Bao, Y., Lai, Q., Lian, X., Li, N., Bao, Y., 2018. Analyzing vegetation dynamic trend on the Mongolian Plateau based on the Hurst exponent and influencing factors from 1982-2013. J. Geog. Sci. 28, 595–610. https://doi.org/ 10.1007/s11442-018-1493-x.
- Tong, L., Liu, Y., Wang, Q., Zhang, Z., Li, J., Sun, Z., Khalifa, M., 2019. Relative effects of climate variation and human activities on grassland dynamics in Africa from 2000 to 2015. Ecol. Inform. 53, 100979. https://doi.org/10.1016/j.ecoinf.2019.100979.
- Turner, M.G., Calder, W.J., Cumming, G.S., Hughes, T.P., Jentsch, A., LaDeau, S.L., Lenton, T.M., Shuman, B.N., Turetsky, M.R., Ratajczak, Z., Williams, J.W., Williams, A.P., Carpenter, S.R., 2020. Climate change, ecosystems and abrupt change: science priorities. Phil. Trans. r. Soc. b. 375, 20190105. https://doi.org/10.1098/rstb.2019.0105.
- Urbach, N., Ahlemann, F., 2010. Structural equation modeling in information systems research using partial least squares. JITTA 11, 5–40. https://aisel.aisnet.org/jitta/vol11/iss2/2.
- Veldman, J.W., Overbeck, G.E., Negreiros, D., Mahy, G., Le Stradic, S., Fernandes, G.W., Durigan, G., Buisson, E., Putz, F.E., Bond, W.J., 2015. Where tree planting and forest expansion are bad for biodiversity and ecosystem services. Bioscience 65, 1011–1018. https://doi.org/10.1093/biosci/biv118.
- Wang, G., Peng, W., Zhang, L., Zhang, J., 2023a. Quantifying the impacts of natural and human factors on changes in NPP using an optimal parameters-based geographical detector. Ecol. Ind. 155, 111018. https://doi.org/10.1016/j.ecolind.2023.111018.

- Wang, Q., Liang, L., Wang, S., Wang, S., Zhang, L., Qiu, S., Shi, Y., Shi, J., Sun, C., 2023b. Insights into Spatiotemporal Variations in the NPP of Terrestrial Vegetation in Africa from 1981 to 2018. Remote Sens. 15, 2748. https://doi.org/10.3390/rs15112748.
- Wang, S., Zhang, Y., Ju, W., et al., 2020. Recent global decline of CO2 fertilization effects on vegetation photosynthesis. Science 370, 1295–1300. https://doi.org/10.1126/ science.abb7772.
- Wang, T., Wang, M., 2015. The Current Situation, Opportunities and challenges of Low-Carbon Development in Africa. J. Southwest Pet. Univ. (soc. Sci. Ed.) 17, 1–9. https://link.cnki.net/urlid/51.1719.c.20150331.1623.015.
- White, F., 1983. The vegetation of Africa: a descriptive memoir to accompany the UNESCO/AETFAT/UNSO vegetation map of Africa. UNESCO, Paris, France, pp. 10–28
- Yadou, B.A., Ntang, P.B., Baida, L.A., 2024. Remittances-ecological footprint nexus in Africa: do ICTs matter? J. Clean. Prod. 434, 139866. https://doi.org/10.1016/j. iclepro.2023.139866
- Yang, Y., Wu, J., Niu, B., Li, M., 2024. Mitigating the negative effects of droughts on alpine grassland productivity in the northern Xizang Plateau via degradationcombating actions. Int. J. Appl. Earth Obs. Geoinf. 134, 104171. https://doi.org/ 10.1016/j.jag.2024.104171.
- Yu, T., Sun, R., Xiao, Z., Zhang, Q., Liu, G., Cui, T., Wang, J., 2018. Estimation of Global Vegetation Productivity from Global Land Surface Satellite Data. Remote Sens. 10, 327. https://doi.org/10.3390/rs10020327.
- Yue, S., Pilon, P., Cavadias, G., 2002. Power of the Mann-Kendall and Spearman's rho tests for detecting monotonic trends in hydrological series. J. Hydrol. 259, 11–24. https://doi.org/10.1016/S0022-1694(01)00594-7.

- Zhang, Q., Tang, H., Cui, F., Dai, L., 2019. SPEI-based analysis of drought characteristics and trends in Hulun Buir grassland. Acta Ecol. Sin. 39, 7110–7123. https://doi.org/10.5846/stxb201807061481.
- Zhang, X., Liu, L., Chen, X., Gao, Y., Xie, S., Mi, J., 2021. GLC\_FCS30: global land-cover product with fine classification system at 30m using time-series Landsat imagery. Earth Syst. Sci. Data 13, 2753–2776. https://doi.org/10.5194/essd-13-2753-2021.
- Zhang, X., Liu, L., Wu, C., Chen, X., Gao, Y., Xie, S., Zhang, B., 2020. Development of a global 30m impervious surface map using multisource and multitemporal remote sensing datasets with the Google Earth Engine platform. Earth Syst. Sci. Data 12, 1625–1648. https://doi.org/10.5194/essd-12-1625-2020.
- Zhao, B., Ma, Z., Li, P., Xu, Y., Zhang, G., Ma, W., Ren, Z., 2023. Drivers of net primary productivity spatio-temporal variation in Ningxia. China. Forests. 14, 1170. https://doi.org/10.3390/f14061170.

#### Further reading

- Deng, X., Hu, S., Zhan, C., 2022. Attribution of vegetation coverage change to climate change and human activities based on the geographic detectors in the Yellow River Basin. China. Environ. Sci. Pollut. Res. 29, 1–16. https://doi.org/10.1007/s11356-022-18744-8.
- Liu, H., Liu, F., Yuan, L., Z. y.,, 2022b. Assessing the relative role of climate and human activities on vegetation cover changes in the up-down stream of Danjiangkou. China. J. Plant Ecol. 15, 180–195. https://doi.org/10.21203/rs.3.rs-184024/v1.
- Liu, L., Zhang, X., Gao, Y., Chen, X., Xie, S., Mi, J., 2021c. Finer-Resolution Mapping of Global Land Cover: recent Developments, Consistency Analysis, and prospects. J. Remote Sens. 3, 1–38. https://doi.org/10.34133/2021/5289697.